Advanced power management algorithm for grid connected hybrid renewable energy system for efficient power sharing

GUTHHI ANUSHA[1] Dr.A.SRUJANA[2]

[1]PG Scholar, VIDYA JYOYHI INSTITUTE OF TECHNOLOGY, Hyderabad, India

[2]Professor, VIDYA JYOYHI INSTITUTE OF TECHNOLOGY, Hyderabad, India

Abstract. This paper presents a hybrid system comprise of PV, Battery, SC, Grid to meet isolated DC load demand. The PV is the primary energy source, whereas battery and SC both are considered for their different power density to supply transient and steady load respectively. The penetration of micro-grid with the distribution system becomes a challenge for the reliable and safe operation of the existing power system. The sporadic characteristics of sustainable energy sources along with the random load variations greatly affect the power quality and stability of the system. Hence, it requires storage systems having both high energy and high-power handling capacity to coexist in micro-grids. An efficient energy management structure is designed in this paper for a grid-united PV system combined with hybrid storage of super-capacitor and battery. The combined battery and super-capacitor storage system grips the average and transient power changes, which provides a quick control for the DC link voltage, i.e., it stabilizes the system and helps to achieve the PV power smoothing. The average power distribution between the power grid and battery is done by checking the SOC of a battery, and an effective and efficient energy management scheme is proposed. Additionally, the use of a super-capacitor lessens the current stress on the battery system during unexpected disparity in the generated power and load requirement. The current controller in the control module is replaced with P&O MPPT technique for maximum power extraction from the PV module. A comparative analysis is done with current control and MPPT control and the results are presented using MATLAB software.

Keywords: PV (Photo Voltaic), SC (Super Capacitor), SOC (State Of Charge), P&O (Perturb and Observe), MPPT (Maximum Power Point Tracking), MATLAB.

1. Introduction

The depletion of fossil fuel and their impact on the environment has resulted in the transition toward renewable energy sources (RES) to overcome the global energy challenges. These RESs are great alternatives to power generation to reduce CO_2 and greenhouse gas emissions [1]. Some of the most prominent RESs are solar photovoltaic (PV), hydro, wind, geothermal, biomass, etc. Due to the low operating cost, easy installation process, and low maintenance, the PV system becomes the most promising technology to cover future energy demands [2]. In recent years, environmental sustainability, efficiency, reliability, robustness, power management, and some power quality features are some of the benefits that are provided by microgrid (MG) technology [3]. A microgrid is basically a controllable power supply system that interconnects with a group of distributed energy resources (DERs) and loads in a defined electrical boundary. It can operate either in islanded/isolated mode or in grid-connected mode [4]. The simple layout of a microgrid with different energy storage devices and utility grids is shown in Figure 1.

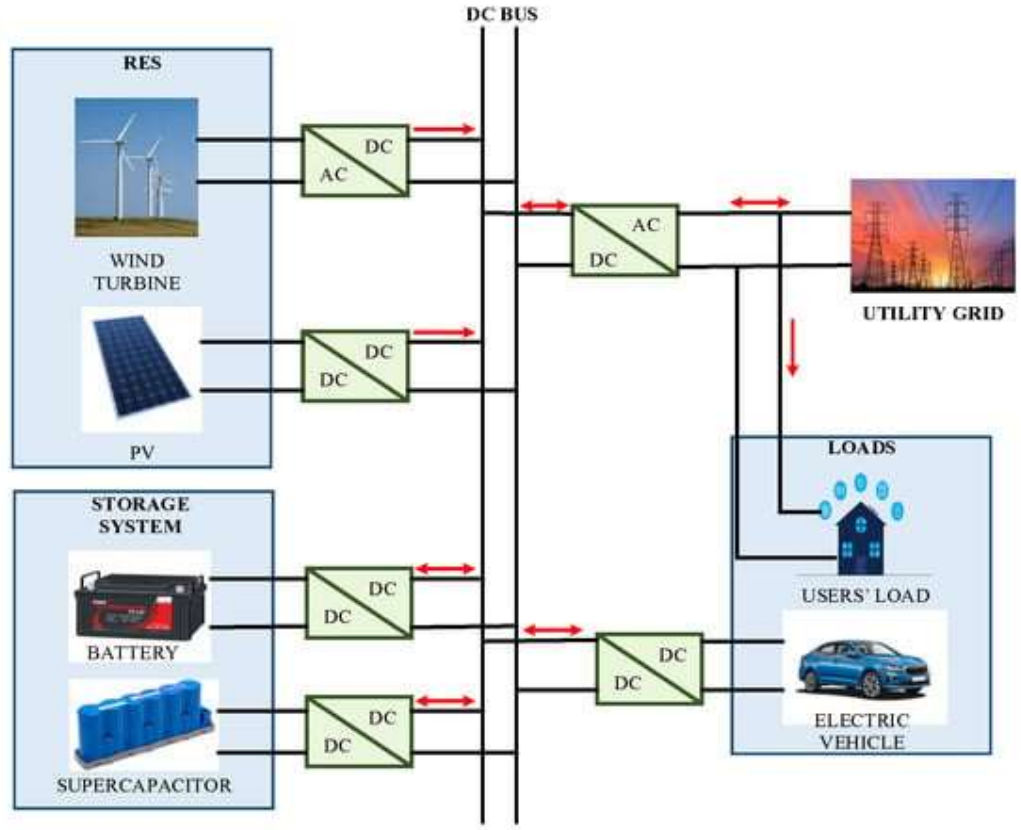

Fig. 1. Outline of a microgrid.

The microgrid can be considered as a small-scale low power supply system, but there are a number of factors that differentiate the microgrid from the existing conventional grids. The intermittent nature of the environment poses new challenges with the use of RESs. The issues with meteorological conditions are the variations in power generation [8]. As a consequence, the power balance between generation and loads, constant power supply to the loads, microgrid stability, and reliability become promising problems in MG operation. To overcome these problems, storage devices are integrated with the microgrid nowadays. Integration of microgrids with storage devices can overcome power fluctuations, regulate the frequency, improve power qualities, and enable some ancillary services [9]. A combination of different energy storage devices with complementary characteristics is taken into consideration to form a hybrid energy storage system (HESS) to overcome the limitations of a single storage system. In most MG applications, the battery storage is integrated with the supercapacitor (SC) storage system to form the composite storage system [10]. The life span of the HESS is a major concern to evade the premature degradation of the devices. Hence, in a HESS, the battery will supply the average power demand of the system and the transient/sudden power requirement of the MG will be supplied by the SC to avoid the deterioration of their life cycle [11].

The combined operation of these RESs, loads, and storage devices in the MG requires a proper control strategy to get the optimal use of the distributed generators (DGs) to feed the connected loads. Hence, a suitable power management strategy is very important for the MG operation [12]. A low-pass filter-based power management study was presented in [10,13,14] to share the total system power requirement between the battery and SC storage system in a PV-integrated hybrid AC/DC microgrid system. In this literature, conventional proportional-integral (PI) controllers are utilized to maintain a

simple control structure. A sliding mode controller-based power management control scheme was proposed in [15] for a PV, wind, and fuel cell with HESS microgrid along with linear and nonlinear loads. In [16], a fixed frequency-based PWM, and in [17], an adjustable bandwidth-based control structure is implemented by using the sliding mode controller to overcome the issues with high and variable frequency-based operation using conventional PI controllers. A battery energy storage-based microgrid was controlled by using the combination of the fuzzy logic controller (FLC) and the DC bus voltage regulation technique in [18]. Here, the state of charge (SOC) and charging/discharging of the battery were properly monitored by the FLC compared to the conventional droop control techniques. A frequency signaling-based fuzzy logic control is utilized in [19] for an islanded AC microgrid with battery energy storage system. For efficient utilization of battery and SC, a multimode fuzzy logic-based power allocation method was proposed in [20]. Nowadays, these power management techniques play very important roles in designing of electric vehicle charging stations [21]. A number of filtering-based techniques, such as the use of rate limiters, high pass filters, low pass filters, and ramp rates, are explained in various works of literature for the management and control of power disparity between generation and demand. In addition, some intelligent control techniques, such as fuzzy logic control, neural network-based controls, and model predictive control (MPC), are used for power management in the MG nowadays.

Different pieces of literature have investigated related to microgrid operations. In various papers, either they focused on different storage devices used in MG or different power management techniques used in microgrid applications. However, in this review article, the analysis is done for different storage devices along with various power management techniques. The main discussion points of this paper are listed below.

(1) Requirement for integration of renewable energy-based microgrid with the existing conventional grids and the operational difference between the microgrid and conventional grid;

(2) Necessity of storage devices in the MG applications and hybridization of two devices by considering different characteristics to get the optimal benefits;

(3) Three types of interconnection topologies, i.e., passive connection, semi-active connection, and active connection of HESS are discussed to increase the system efficiency and reduce the cost;

(4) Comparison of several classical and intelligent approaches for power management in the microgrid with their advantages and limitations are explained;

(5) Finally, various recent trends in power management strategies are compared in AC/DC microgrids.

This rest of this paper is arranged as follows. Section II briefly explains the system architecture and power management scheme. The control structures for converters are described in Section III. The simulation results and discussion are presented in Section IV. Finally, Section V provides the conclusion.

2. System architecture

Hybrid energy storage (HES) results from the integration of two or more different storage technologies into a system. This way, a combination of the advantages and characteristics of different storage methods is performed to achieve specific requirements and improve the whole system performance. The combination of energy and power rating, life cycle, duration of discharge period and other characteristics may not be satisfied by the single storage technology. Supercapacitors have high power rate and short discharge duration, but limited energy density. On the other hand, batteries have high

energy rates and long duration of storage, but limited power. Therefore, this hybridization provides high energy and power rating, fast response and both short and long discharge duration. Moreover, supercapacitors can reduce stress on batteries and increase the battery's life [3], [4].

There are many researchers who propose the use of batteries and supercapacitors together. This combination offers high storage capacity and a very fast response time [5]. Some of them proposed the integration of battery-supercapacitor storage into a wind power plant [6], in an electric vehicle [7] or in a microgrid [8]. Kanchev et al. [9] proposed an energy management method in a building with PV system and a battery-supercapacitor storage. Specifically, excess energy from photovoltaics is stored in batteries and the local real-time power control is achieved by supercapacitors. Therefore, it is necessary to choose an appropriate combination of energy storage systems to follow the system requirements.

As proposed in section I, the distribution network is introduced with three DG units at buses 1, 3, and 4 for local power sharing. Bus 1 is integrated with the PV-Battery-SC module controlled by the PMA algorithm [7]. A wind farm is integrated into bus 3 which uses PMSG (Permanent Magnet Synchronous Generator) for standalone power generation. Bus 4 is interconnected with a fuel cell module where hydrogen is the major source generation of power. All these three DG units are operated in synchronization with the grid by control [8] of the 3-ph inverter with SRF control structure. The SRF control structure needs feedback on the DC link voltage at the DC side of the inverter, the 3-ph voltages of the grid, and the 3-ph injected currents of the inverter. The SRF controller is integrated with PLL (Phase Locked Loop) which is the vital module for the synchronization of the inverters [9]. The PLL ensures the inverters operate at the same phase and frequency as that of the main grid. With the synchronization control, the power from these DG units is shared with the loads with parallel support of the grid.

In the PMSG wind farm DG unit power extraction is done by a Diode Bridge rectifier (DBR) connected single switch buck-boost converter. The DBR rectifies the AC voltages of the PMSG to unstable DC voltage. The DC stabilization with the required voltage magnitude is achieved by the single switch buck-boost converter controlled by MPPT (maximum power point tracking) algorithm [10]. This DG unit is a grid-dependent source that cannot be operated in standalone mode as the power generation is dependent on unpredictable wind speeds. The DG unit on bus 4 is a fuel cell module operated with a booster converter controlled by voltage feedback control for voltage stabilization. This renewable source is a restricted DG unit that can support only a part of the load and needs interconnection with the grid. The fuel cell DG unit is also a dependent source and cannot be operated in standalone mode with heavy loads connected.

For the standalone operation of the DG unit in a distribution network, the renewable source needs a backup storage device [11] that can support the load during deficit power conditions. The bus 1 DG unit which is the PV source is integrated with a battery and SC-connected two-switch bidirectional converters. The charge and discharge of the battery and SC modules are controlled by the bidirectional converters. The bidirectional converter switches are controlled by the PMA module with feedback taken from PV power, $SOC_{b,}$ and SOC_{sc}. The charge and discharge state of the converter depends on the excess or deficit power availability of the PV power [12]. The complete updated internal circuit structure of the PV DG1 unit can be observed in figure 2.

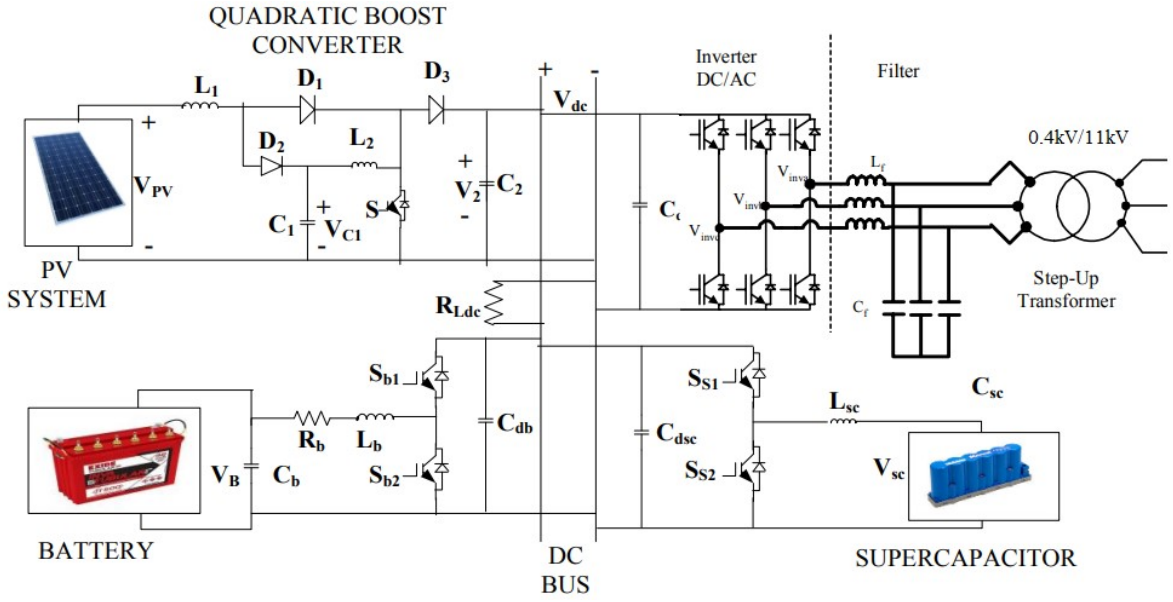

Fig. 2: DG1 PV source module with battery and SC support

For maximum and efficient power extraction from the PV source, the conventional boost converter is replaced with a quadratic boost converter which is controlled by the P&O MPPT algorithm. The two switches in the bidirectional converters (Sb1 Sb2 and Ss1 Ss2) duty ratios are controlled by PMA control. As per the duty ratio of the switches, the charge-discharge of the battery and SC units is decided [13]. The converter operates in buck mode during charging conditions and in boost mode during discharge conditions. All the modules are connected in parallel at the DC bus which injects the combined power into the grid by DC/AC inverter [14] through an LC filter. The inverter is operated by an SRF controller during grid-connected mode and during the standalone mode, it is controlled by a simple Sin PWM technique with no feedback.

3. PMA modelling

The PMA algorithm is the primary control structure of DG 1 placed at Bus 1 which manages the charge and discharge of the battery and SC modules. The PMA control structure generates a duty ratio for the buck and boosts switches of the bidirectional converters connected to the battery and SC. It considers the PV power generated, load demand power, battery SOC and SC SOC [16] for the control of the switches. The complete control structure of the PMA algorithm with feedback parameters can be observed in figure 3.

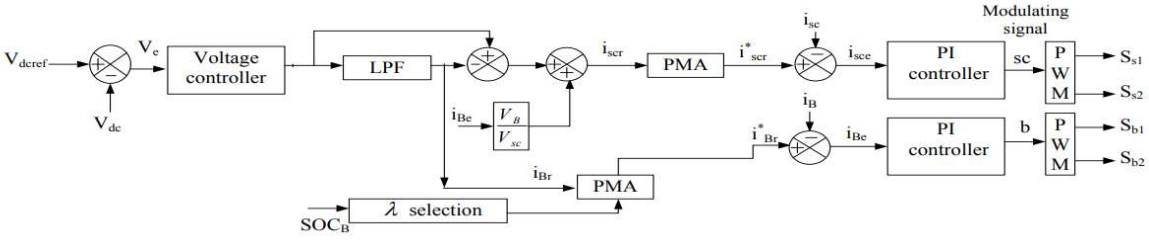

Fig. 3: PMA control structure for control of battery and SC

In the given control structure the V_{dcref} is the required reference DC voltage on the DC side of the 3-ph inverter and V_{dc} is the measured DC voltage of the same. The comparison of these voltages generates voltage error V_e fed to PI voltage controller generating i_t (required current). It is expressed as

$$i_t = K_p V_e + K_i \int V_e dt \quad (1)$$

For the reduction of disturbances in the current signal, an LPF (Low Pass Filter) is utilized [17]. The feed-forward comparison of the LPF signal and the previous signal generates high order harmonics signal $\overline{i_{Br}}$. The higher order harmonics signal is used for the generation of SC reference current i_s given as

$$i_{scr} = \overline{i_{Br}} + i_{Be} \frac{V_B}{V_{SC}} \quad (2)$$

Here, i_{Be} is the measured battery current, V_B is the battery voltage and V_{SC} is the SC voltage. Both the current reference signals i^*_{scr} and i^*_{Br} are generated by the PMA which depends on λ selection. The λ depends on the SOC of the battery which is determined by table 1.

Table 1: λ selection table

SOC_b	**λ**
0.8< SOC_b <0.95	1
0.45< SOC_b <0.8	0.6
0.15< SOC_b <0.45	0.3
SOC_b <0.15	0

As per the given table 1 the value of λ varies from 0-1 concerning SOC_b. Now as per the λ value, i_{scr} and i_{Br} the reference battery and SC currents (i^*_{scr} and i^*_{Br}) are calculated as per the given table 2.

Table 2: PMA concerning PV power availability

Insufficient Power mode	
SOC range	*Reference currents*
SOC_b > L ; SOC_{sc} > L	$i^*_{Br} = \lambda i^*_t$; $i^*_{scr} = i'_t$
SOC_b < L ; SOC_{sc} > L	$i^*_{Br} = 0$; $i^*_{scr} = i'_t$
SOC_b > L ; SOC_{sc} < L	$i^*_{Br} = \lambda i^*_t$; $i^*_{scr} = 0$
SOC_b < L ; SOC_{sc} < L	$i^*_{Br} = 0$; $i^*_{scr} = 0$
Sufficient and Floating Power mode	
SOC range	*Reference currents*
SOC_b < U ; SOC_{sc} < U	$i^*_{Br} = i_{B.ch}$; $i^*_{scr} = i_{SC.ch}$
SOC_b < U ; SOC_{sc} > U	$i^*_{Br} = i_{B.ch}$; $i^*_{scr} = i'_t$

$SOC_b > U$; $SOC_{sc} < U$	$i_{Br}^* = 0$; $i_{scr}^* = i_{SC.ch}$
$SOC_b > U$; $SOC_{sc} > U$	$i_{Br}^* = 0$; $i_{scr}^* = i_t'$

In the above-given table 2 the 'L' and 'U' are the lower and upper limits of SOC respectively taken as 0.15 and 0.95. The considered currents are expressed as

$$i_t^* = \frac{w_c}{s+w_c}\, i_t \qquad (3)$$

$$i_t' = \left(1 - \frac{w_c}{s+w_c}\right) i_t \qquad (4)$$

$$i_{B.ch} = \frac{-P_{Br}}{V_B} \qquad (5)$$

$$i_{SC.ch} = -P_{sc}\sqrt{\frac{C_{sc}}{2E_{sc}}} \qquad (6)$$

In the above given current equations 'w_c' LPF cutoff frequency (2*pi*10), P_{Br} is the power of the battery, P_{sc} is the power of SC, C_{sc} is SC capacitance and E_{sc} is the Energy stored in SC. Therefore as per the given PMA table and current expressions the reference currents i_{scr}^* and i_{Br}^* are generated as per PV power availability (Sufficient, Insufficient or Floating) [18]. These reference currents are compared to measured SC current i_{sc} and battery current i_{Br} and the error signals are fed to current PI controllers. The individual current controllers generate a duty ratio fed to the PWM generator generating signals for bidirectional converter switches controlling the charging and discharging currents of the battery and SC. The design and modeling of the configured modules are done in the next section with results generated as per the given operating conditions.

4. Simulation results

The architecture of the grid coupled PV system with storage devices is presented in Fig. 4. To get the required DC link voltage, the output voltage of DC-DC converter should be sufficiently high for the integration of a low-voltage PV system with the distribution system. Hence, a quadratic boost converter is used with a PV system to get a high conversion ratio with high efficiency for a wide range of voltage. For energy storage, super-capacitors and batteries are utilized along with the bidirectional boost DC-DC converter (BDDC) for the regulation of power transfer among the grid and the ESSs.

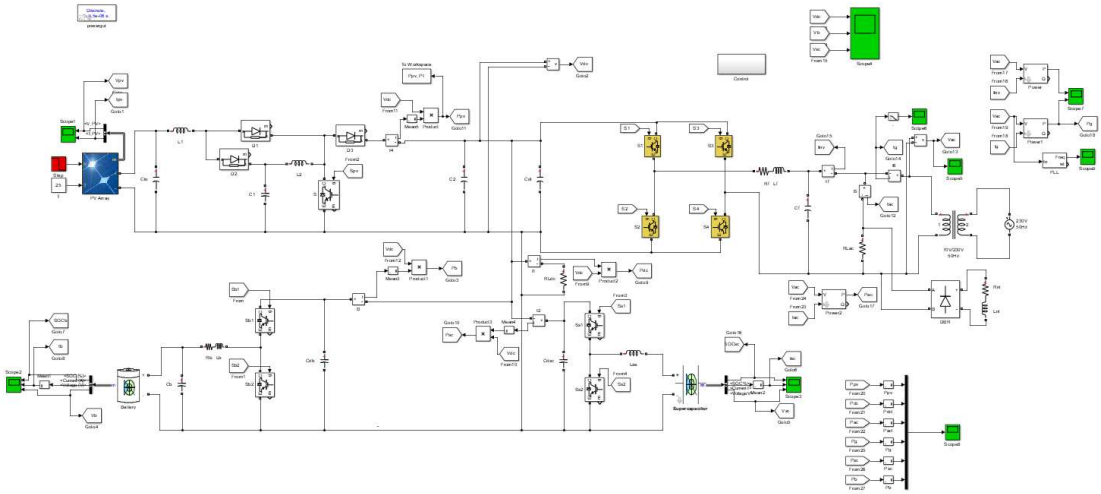

Fig. 4: Modelling of proposed test system

The AC utility grid is linked to the DC micro-grid via a voltage source converter (VSC), which can operate as an inverter or a rectifier according to the mode of operation. The LC filter is used at the output of VSC to smooth the voltages and currents at the AC side. In this system, both linear and nonlinear loads are connected to check the performance of the proposed scheme under different operating conditions. The below is the modeling of proposed controller scheme to control the converters of the test system.

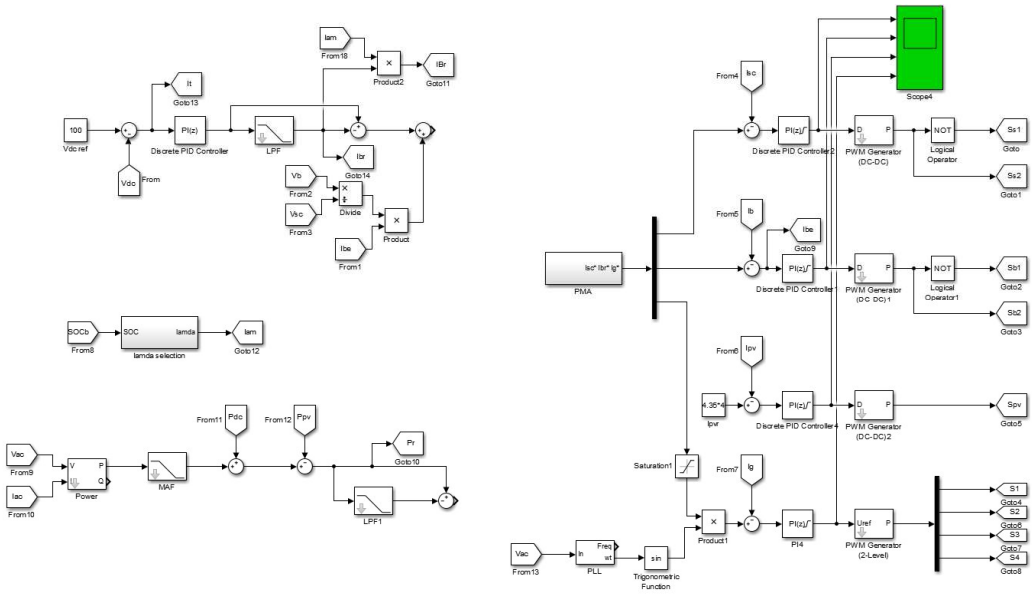

Fig. 5: Control structure modelling

This power management structure mainly comprises the generation of reference current, an algorithm for power management, control of various currents converters. Depending on the PV generation and load requirement, the power management algorithm (PMA) selects the mode of operation and produces the current references. Then, these reference currents under-

go the current control stages and finally, produce the switching pulses for all the power converters.

TABLE I
LOGIC FOR λ IN INSUFFICIENT POWER MODE [18]

$SOC_b(t)$	λ	$1-\lambda$
$0.7<SOC_b<U$	1	0
$0.5<SOC_b<0.7$	0.6	0.4
$0.1<SOC_b<0.5$	0.3	0.7
$SOC_b<L$	0	1

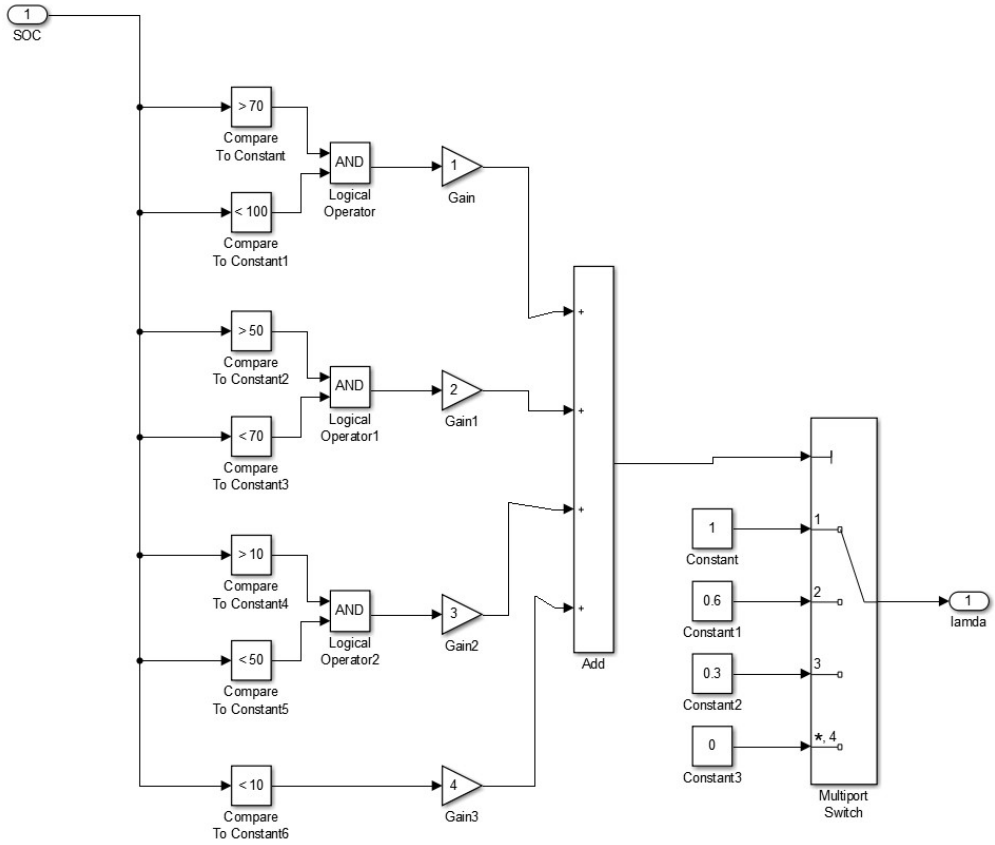

Fig. 6: Lamda selection with respect to SOC of battery

The above is the modeling of lamda value generation with respect to SOC of the battery as per the given reference table. The active performance of the planned control strategies under the condition of variation of PV power generation is shown in below figures. The PV power generation is varied at t=2 s by changing the irradiance of the system from 1000 W/m2 to 700 W/m2. The reduction in PV generation at 2 s is noticeable. Irrespective of the change in PV power, the DC bus voltage regains its constant voltage value at 100V.

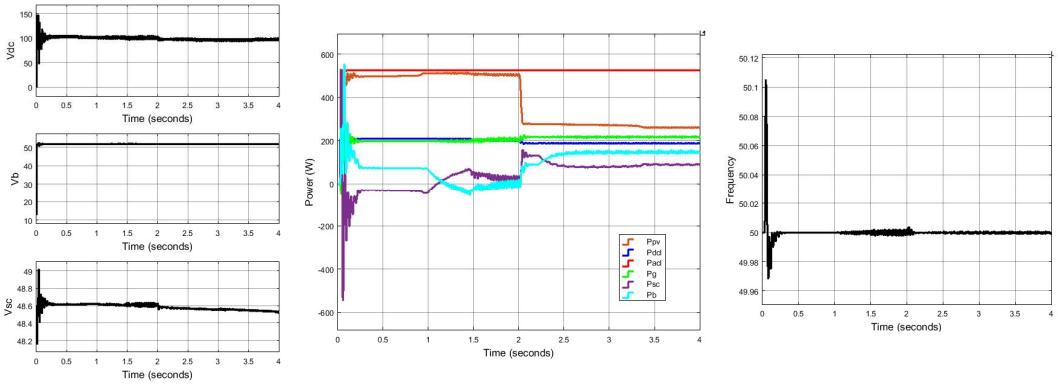

Fig. 7: Vdc, Vb, Vsc, powers of all modules PV, DC load, AC load, Grid, SC, battery and frequency of grid during PV power variation at 2sec.

At the point of change, the transient power surge is handled by the supercapacitor unit. The average component is compensated by the battery units and grid combinedly and preserves the constant DC link voltage. The combination of battery with supercapacitor effectively reduces the settling time and voltage dip at the point of PV generation change. As the settling time is reduced, the vicinity of the final val- ue of the DC bus voltage is reached very quickly within the specified error.

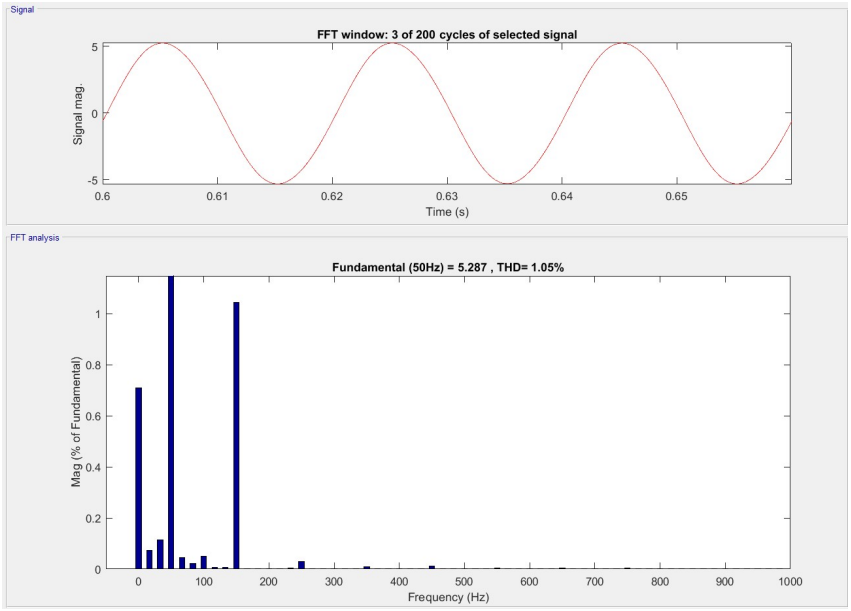

Fig. 8: THD of grid current during PV power variation

The total harmonic distortion (THD) with variation in PV power generation is shown in Fig. 8. It is clearly visible from Fig. 8 that THD of utility grid current is 1.05%, which is within the acceptable THD range according to IEEE std. 519.

The performance of the proposed control strategies under the condition of load variation is shown in Fig 9, and it is tested under insufficient power conditions. The DC load increases at t=2 s by varying the linear DC load from RLdc = 50Ω to RLdc = 25 Ω. The abrupt variation in DC load power at t=2 s is visible in Fig. 9. The average power demand to make the DC bus

voltage persistent is handled by the power grid and the batteries and the transient power are handled by the super-capacitor.

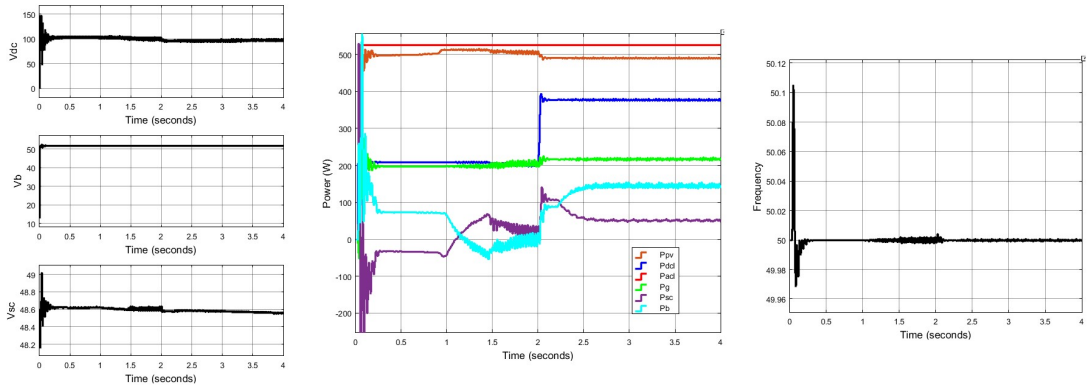

Fig. 9: Vdc, Vb, Vsc, powers of all modules PV, DC load, AC load, Grid, SC, battery and frequency of grid during DC load power variation at 2sec.

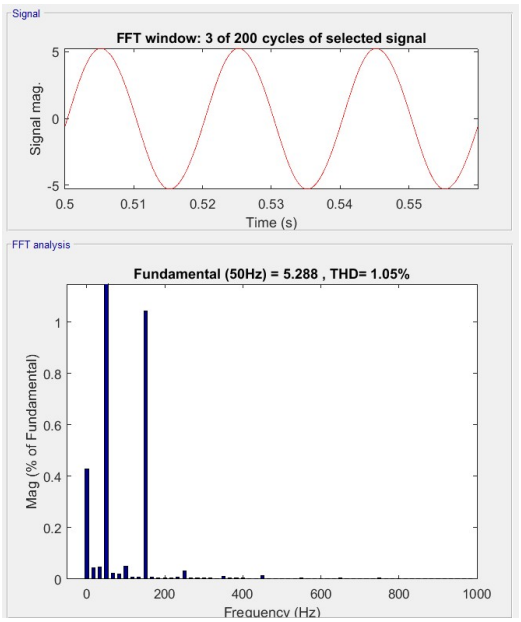

Fig. 10: THD of grid current during DC load power variation

When SOCb < L and SOCsc < L, both battery and supercapacitor become idle. The total shortage of power demand is provided by the power grid only to make the DC link voltage constant. Irrespective of any state in IPM, the DC bus voltage restores very quickly.

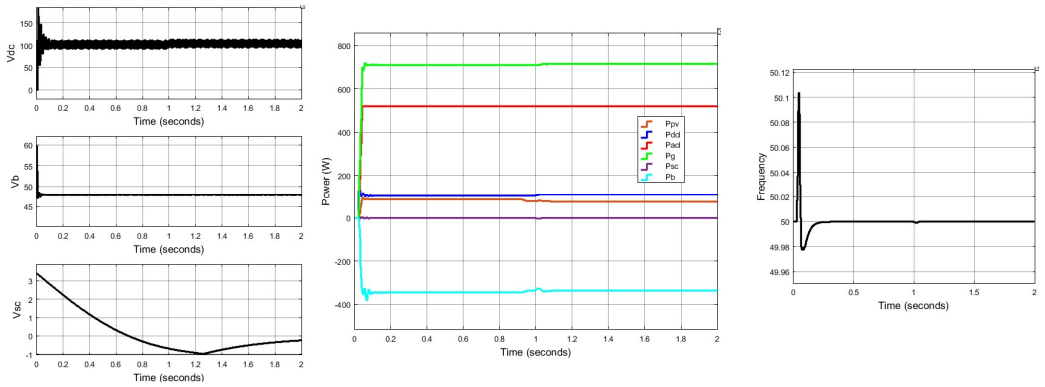

Fig. 11: Vdc, Vb, Vsc, powers of all modules PV, DC load, AC load, Grid, SC, battery and frequency of grid during IPM condition with SOCb < 10 and SOCsc < 10.

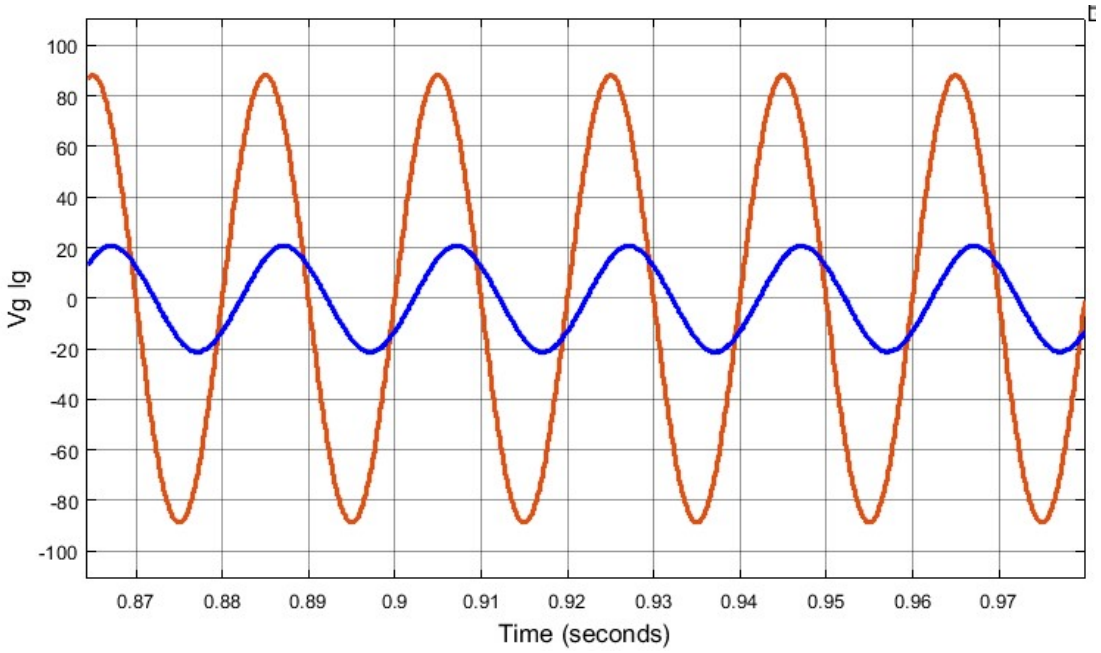

Fig. 12: Grid power inverter power and grid voltage current during IPM condition

When SOCb < U and SOCsc < U, the battery, and the super-capacitor are charged based on their respective rated charging current. After charging the storage devices, the remaining excess power is supplied to the power grid.

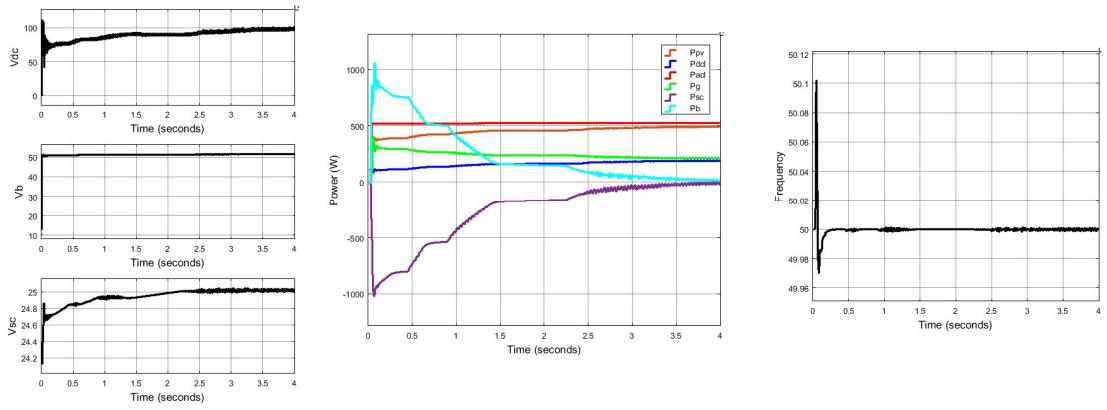

Fig. 13: Vdc, Vb, Vsc, powers of all modules PV, DC load, AC load, Grid, SC, battery and frequency of grid during SPM condition with 10 < SOCb < 70 and 10 < SOCsc < 70.

The proposed controller is updated with P&O MPPT replacing the conventional current PI controller for maximum power extraction. The below fig. 14 is the update modeling of the controller.

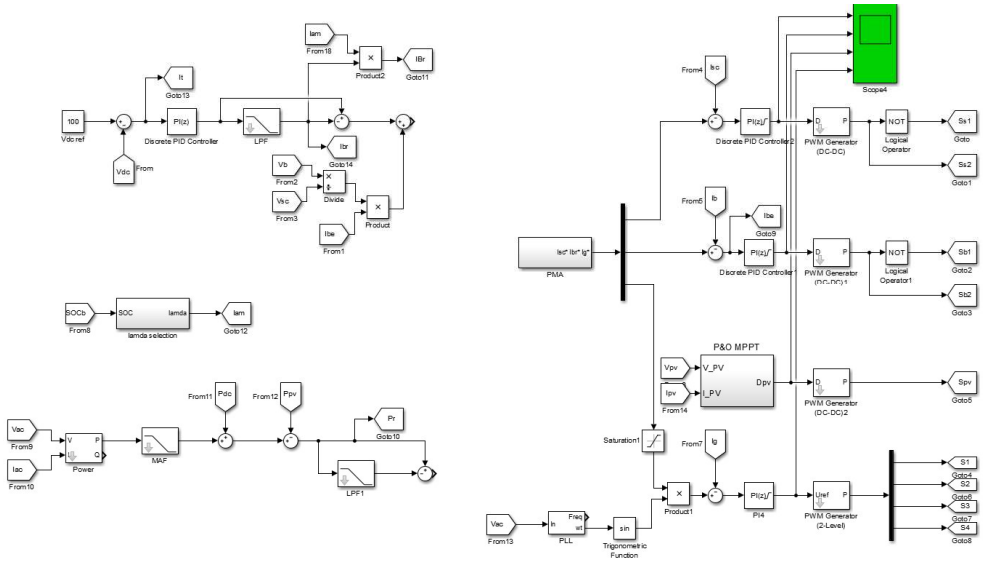

Fig. 14: Updated control structure with P&O MPPT control

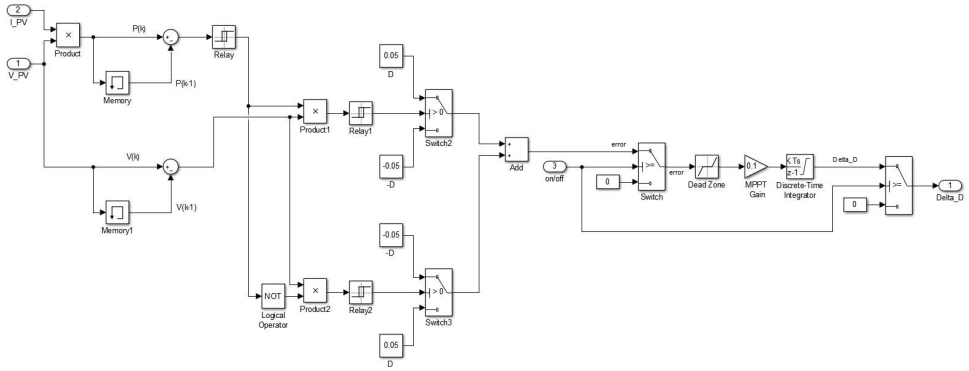

Fig. 15: P&O MPPT algorithm modeling

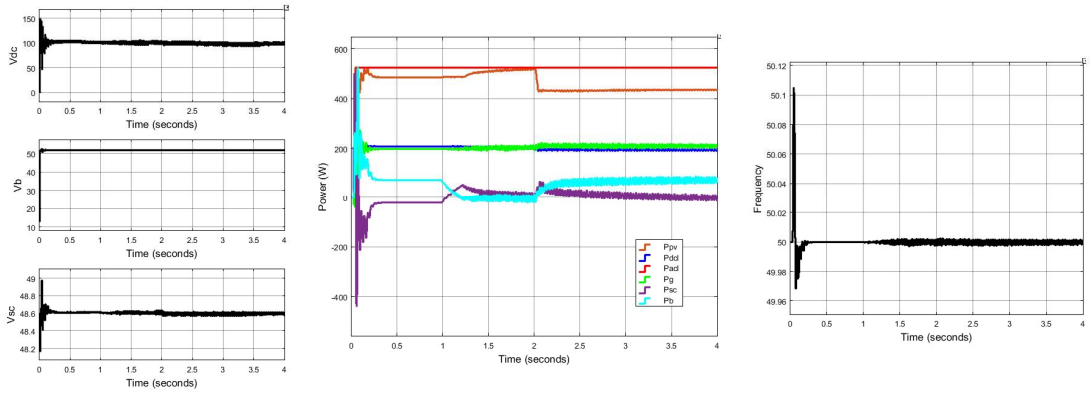

Fig. 16: Vdc, Vb, Vsc, powers of all modules PV, DC load, AC load, Grid, SC, battery and frequency of grid with MPPT control of PV module and PV power variation

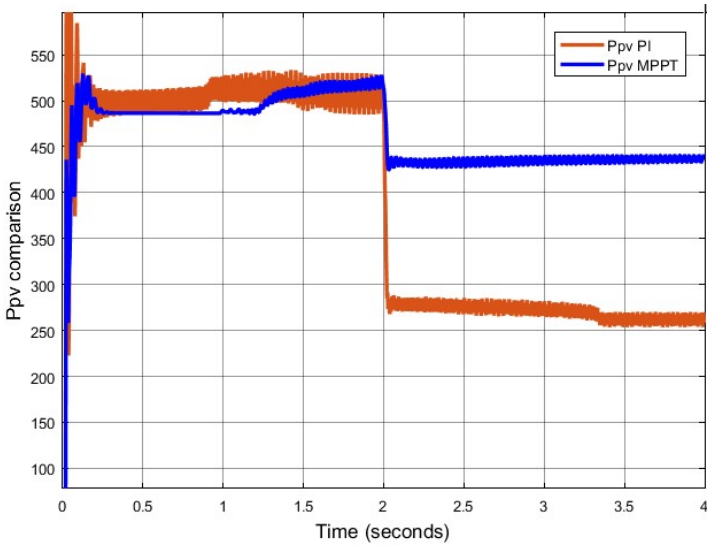

Fig. 17: PV power comparison with PI and MPPT controllers

As it can be seen that the power from PV extracted during drop in irradiation is higher when operated with MPPT control.

5. Conclusion

The objectives of the proposed scheme, e.g., faster DC volt- age regulation, voltage and frequency regulation, maintenance of power quality issues, and limiting the SOC of storage systems within their limits, are justified through simulation results. The potency of the discussed control technique is conveyed by comparing the power quality features like settling time, overshoot/undershoot, and THD with other different methods. The drop in power with PI controller is from 500W to 250W and with MPPT control it dropped from 500W to 430W. Therefore, the MPPT control updated has better performance as compared to PI controller.

References

[1] S. K. Kollimalla and M. K. Mishra, “A novel adaptive P&O MPPT al- gorithm considering sudden changes in the irradiance,” IEEE Transac- tions on Energy Conversion, vol. 29, no. 3, pp. 602-610, May 2014.

[2] S. Mishra and R. K. Sharma, “Dynamic power management of PV based islanded microgrid using hybrid energy storage,” in Proceedings of IEEE 6th International Conference on Power Systems (ICPS), New Delhi, India, Mar. 2016, pp. 1-6.

[3] C. Natesan, S. Ajithan, S. Chozhavendhan et al., “Power management strategies in microgrid: a survey,” International Journal of Renewable Energy Research, vol. 5, no. 2, pp. 334-340, Jan. 2015.

[4] Z. Yi, W. Dong, and A. H. Etemadi, “A unified control and power management scheme for PV-battery-based hybrid microgrids for both grid-connected and islanded modes,” IEEE Transactions on Smart Grid, vol. 9, no. 6, pp.5975-5985, Nov. 2018.

[5] S. Pannala, N. Patari, A. K. Srivastave et al., “Effective control and management scheme for isolated and grid connected DC microgrid,” IEEE Transactions on Industry Applications, vol. 56, no. 6, pp. 1-14, Dec. 2020.

[6] P. Singh and J. S. Lather, “Variable structure control for dynamic pow- er-sharing and voltage regulation of DC microgrid with a hybrid ener- gy storage system,” International Transaction Electrical Energy Sys- tem, vol. 30, no. 9, pp. 1-20, Jun. 2020.

[7] N. R. Tummuru, U. Manandhar, A. Ukil et al., “Control strategy for AC-DC microgrid with hybrid energy storage under different operat- ing modes,” Electrical Power and Energy Systems, vol. 104, pp. 807-816, Jan. 2019.

[8] J. Hu, Y. Shan, Y. Xu et al., “A coordinated control of hybrid AC/DC microgrids with PV-wind-battery under variable generation and load conditions,” Electrical Power and Energy Systems, vol. 104, pp. 583-592, Jan. 2019.

[9] H. Mahmood, D. Michaelson, and J. Jiang, “A power management strategy for PV/battery hybrid systems in islanded microgrids,” IEEE Journal of Emerging and Selected Topics in Power Electronics, vol. 2, no. 4, pp. 870-882, Jun. 2014.

[10] P. Sanjeev, N. P. Padhy, and P. Agarwal, “Peak energy management us- ing renewable integrated DC microgrid,” IEEE Transactions on Smart Grid, vol. 9, no. 5, pp. 4906-4917, Sept. 2018.

[11] S. Sahoo, S. Mishra, and N. P. Padhy, “A decentralized adaptive droop-based power management scheme in autonomous DC mi- crogrid,” in Proceedings of IEEE PES Asia-Pacific Power and Energy Conference, Xi’an, China, Dec. 2016, pp. 1018-1022.

[12] P. Singh and J. S. Lather, “Power management and control of a grid-independent DC microgrid with hybrid energy storage system,” Sus- tainable Energy Technologies and Assessments, vol. 43, pp. 1-11, Feb. 2021.

[13] IEEE Std 929-2000, “IEEE Recommended Practice for Utility Inter-face of Photovoltaic (PV) System”, 2000.

[14] R. Kadri, J. P. Gaubert, G. Champenois et al., “Performance analysis of transformerless single switch quadratic boost converter for grid-con- nected photovoltaic systems,” in Proceedings of International Confer- ence on Electrical Machines (ICEM), Rome, Italy, Sept. 2010, pp. 1-7.

[15] M. Hamzeh, A. Ghazanfari, Y. A. R. I. Mohamed et al., “Modelling and design of an oscillatory current sharing control strategy in DC mi- crogrids,” IEEE Transactions on Industrial Electronics, vol. 62, no. 11, pp. 6647-6657, Nov. 2015.

[16] B. Singh, D. T. Shahani, and A. K. Verma, “IRPT based control of a 50kW grid interfaced solar photovoltaic power generating system with power quality improvement,” in Proceedings of 4th IEEE Internation- al Symposium on Power Electronics for Distributed Generation Sys- tem (PEDG), Rogers, USA, Apr. 2014, pp. 1-8.

[17] S. Golestan, M. Ramezani, J. Guerrero et al., “Moving average filter-based phase-locked loops: performance analysis and design guide- lines,” IEEE Transactions on Power Electronics, vol. 29, no. 6, pp. 2750-2763, Jun. 2014.

[18] N. R. Tummuru, M. K. Mishra, and S. Srinivas, “Dynamic energy management of renewable grid integrated hybrid energy storage sys- tem,” IEEE Transactions on Industrial Electronics, vol. 62, no. 12, pp. 7728-7737, Dec. 2015.

[19] H. Wang, Z. Wu, G. Shi et al., “SOC balancing method for hybrid en- ergy storage system in microgrid,” in Proceedings of 3rd IEEE Inter- national Conference on Green Energy and Applications, Taiyuan, Chi- na, Oct. 2019, pp. 141-145.

[20] H. Bindner, T. Cronin, P. Lundsager et al., “Lifetime Modelling of Lead Acid Batteries”, Risø-R-1515(EN), 2005.

[21] IEEE 519-1992- IEEE Recommended Practices and Requirements for Harmonic Control in Electrical Power Systems.

[22] S. Kotra and M. K. Mishra, “A supervisory power management sys- tem for a hybrid microgrid with HESS,” IEEE Transactions on Indus- trial Electronics, vol. 64, no. 5, pp. 3640-3649, May 2017.